



OPEN ACCESS

EDITED BY
Sajjad Gharaghani,
University of Tehran, Iran

REVIEWED BY
Elena Cichero,
University of Genoa, Italy
Alexander Tikhomirov,
Russian Academy of Medical Sciences,
Russia

*CORRESPONDENCE
Yang Zhou,
✉ yangzhpathology@163.com
Yuanqian Qu,
✉ yuanqian0519@163.com

[†]These authors have contributed equally to this work

SPECIALTY SECTION
This article was submitted to
Experimental Pharmacology and Drug
Discovery,
a section of the journal
Frontiers in Pharmacology

RECEIVED 10 November 2022
ACCEPTED 12 December 2022
PUBLISHED 22 December 2022

CITATION
Wang Y, Zhang H, Li J, Niu M-M, Zhou Y
and Qu Y (2022), Discovery of potent
and noncovalent KRAS^{G12D} inhibitors:
Structure-based virtual screening and
biological evaluation.
Front. Pharmacol. 13:1094887.
doi: 10.3389/fphar.2022.1094887

COPYRIGHT
© 2022 Wang, Zhang, Li, Niu, Zhou and
Qu. This is an open-access article
distributed under the terms of the
[Creative Commons Attribution License
\(CC BY\)](https://creativecommons.org/licenses/by/4.0/). The use, distribution or
reproduction in other forums is
permitted, provided the original
author(s) and the copyright owner(s) are
credited and that the original
publication in this journal is cited, in
accordance with accepted academic
practice. No use, distribution or
reproduction is permitted which does
not comply with these terms.

Discovery of potent and noncovalent KRAS^{G12D} inhibitors: Structure-based virtual screening and biological evaluation

Yuting Wang^{1†}, Hai Zhang^{2†}, Jindong Li³, Miao-Miao Niu¹,
Yang Zhou^{4*} and Yuanqian Qu^{4*}

¹Department of Pharmaceutical Analysis, China Pharmaceutical University, Nanjing, China, ²Department of Hepatobiliary Surgery, The Affiliated Hospital of Jiangsu University, Zhenjiang, China, ³Institute of Clinical Medicine, Department of Pharmacy, The Affiliated Taizhou People's Hospital of Nanjing Medical University, Taizhou, China, ⁴Department of Pathology, Department of Gastrointestinal Surgery, The Affiliated Changzhou Second People's Hospital of Nanjing Medical University, Changzhou, China

KRAS^{G12D}, the most common oncogenic KRAS mutation, is a promising target for the treatment of pancreatic cancer. Herein, we identified four potent and noncovalent KRAS^{G12D} inhibitors (hits 1–4) by using structure-based virtual screening and biological evaluation. The *in vitro* assays indicated that the four compounds had sub-nanomolar affinities for KRAS^{G12D} and showed a dose-dependent inhibitory effect on human pancreatic cancer cells. In particular, the hit compound 3 was the most promising candidate and significantly inhibited the tumor growth of pancreatic cancer in tumor-bearing mice. The hit compound 3 represented a promising starting point for structural optimization in hit-to-lead development. This study shows that hit compound 3 provides a basis for the development of the treatment of cancer driven by KRAS^{G12D}.

KEYWORDS

KRAS^{G12D}, pancreatic cancer, inhibitor, virtual screening, biological evaluation

1 Introduction

Pancreatic cancer is one of the most invasive diseases with almost the same mortality in many countries (Elsayed and Abdelrahim, 2021; Sung et al., 2021). It has the lowest 5-year survival rate of 7% among cancer types (Ducreux et al., 2015; Zhou et al., 2018). The low early diagnosis rate and strong therapeutic resistance largely limit the effective treatment of patients with pancreatic cancer. Most of the patients were already in the unresectable stage at the time of diagnosis. In addition, the tumor is resistant to all forms of routine clinical treatment. It is estimated that pancreatic cancer will become the second leading cause of cancer-related deaths by 2030 (Bazhin et al., 2014; Busato et al., 2022), which highlights the need to develop new treatment drugs to improve the survival rate of patients with pancreatic cancer.

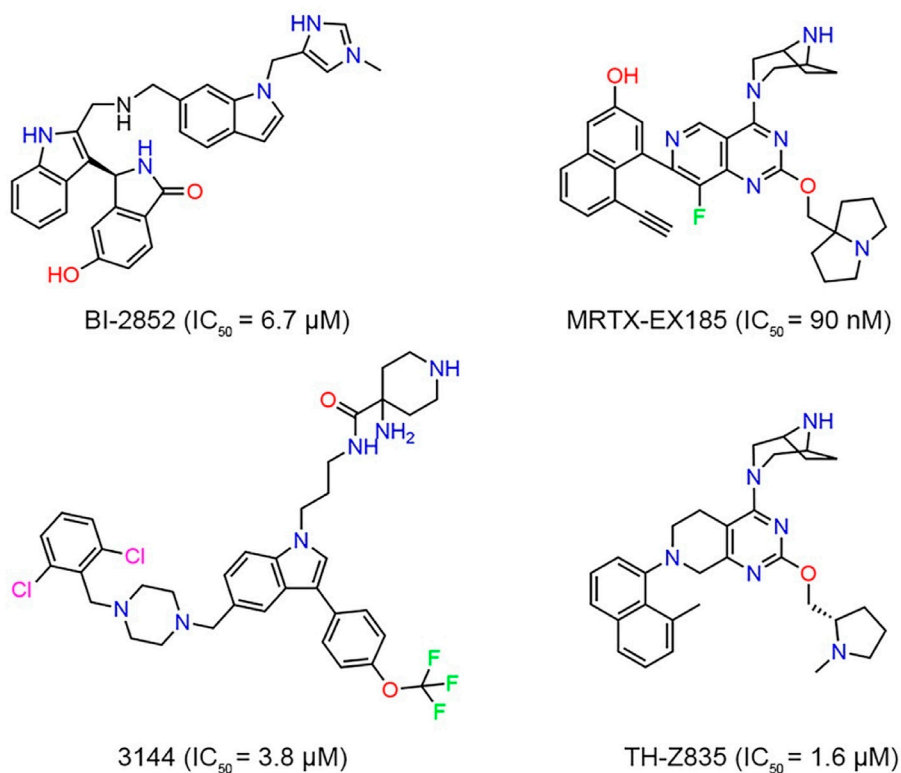


FIGURE 1
The chemical structures and biological data of known inhibitors of KRAS^{G12D}.

KRAS (Kirsten Ras protein) was found to be the most common locus for somatic gain-of-function mutations in patients with pancreatic cancer, accounting for about 95% (Morris et al., 2010; Eibl and Rozengurt, 2019). Recent studies have revealed that mutated KRAS expression is associated with reduced anticancer activity of gemcitabine and paclitaxel, the drugs currently used in the clinical treatment of pancreatic cancer, and new therapeutic strategies of targeting KRAS should inhibit tumor cell growth and combat drug resistance (Kimmelman, 2015; Grasso et al., 2017). The majority of cancer-associated hotspot mutations occur at codons G12, G13, and Q61, wherein G12 represents the most common mutation site (Kargbo, 2022). Among dominant mutations at G12, G12D has the highest mutation frequency (35.4%), followed by G12V (23.5%), G12R (8.7%) and G12C (4.3%), which has aroused the interest of many drug researchers in developing new cancer treatment methods targeting KRAS^{G12D} mutant (Salem et al., 2021). Mutations in RASA, the central signal transduction molecule, directly impair the intrinsic GTPase activity of KRAS and prevent the GTPase activating protein (GAP) from promoting the conversion of active GTP to inactive GDP (Wang et al., 2021). KRAS proteins then bind to GTP and activate downstream effector proteins and signaling pathways

(mechanistic targets of mitogen-activated protein kinase (MAPK) -MAPK kinase (MEK) and phosphatidylinositol 3-kinase (PI3K) -Akt-rapamycin (mTOR)), leading to sustained cell proliferation (Buscail et al., 2020; Zheng et al., 2022). Therefore, targeting KRAS^{G12D} has the potential to block the occurrence and development of pancreatic cancer from the source.

Although KRAS^{G12D} is an excellent drug discovery target for many cancers, no drug directly targeting KRAS^{G12D} has been clinically approved. Targeting the KRAS^{G12D} mutation with a small molecule still remains a challenge due to lack of druggable pockets on the surface of RAS (Cox et al., 2014; Simanshu et al., 2017). However, with the study of RAS binding to low-molecular-weight organic molecules and the recent FDA approval of AMG 510 (Lumakras), a KRAS^{G12C} inhibitor binding to GDP, there has been a resurgence of research surrounding RAS (Chen et al., 2020; Lanman et al., 2020). Investigators reported a structural-designed KRAS inhibitor (BI-2852) that bound to the shallow pocket between switches I and II of KRAS^{G12D} and inhibited the protein-protein interaction between GDP-bound KRAS and SOS (Figure 1). However, limited cellular activity was observed (Kessler et al., 2019; Chen et al., 2020). Vasta et al. (2022) used the NanoBiT

protein-protein interaction assay to evaluate the inhibitory effect of MRTX-EX185 on KRAS^{G12D} in cells and demonstrated that MRTX-EX185 is a potent KRAS^{G12D} inhibitor, albeit with low affinity. Welsch et al. designed a small molecule compound, named 3144, had affinity in the micromolar range, but toxicity and off-target activity of compound 3144 were detected in cells and mice, in addition, its low water solubility made it difficult to use in some contexts (Welsch et al., 2017; Khan et al., 2020). TH-Z835 was designed based on salt-bridge and induced fit pocket formation for KRAS^{G12D} targeting and inhibited the proliferation of cancer cells and significantly reduced the tumor volume. However, THZ835 had an off-target effect because the inhibition was not fully dependent on KRAS mutation status (Mao et al., 2022).

At present, the drug molecules with KRAS^{G12D} protein inhibitory activity reported have made slow progress in research and development (He et al., 2022). The novel molecular skeleton can provide more possibilities for specific effects or clinical studies, so it is necessary to study the new molecular skeleton of KRAS^{G12D} inhibitors (Peng et al., 2018). Molecular modeling of compound databases and virtual screening based on docking are one of the effective technologies to discover new chemical bioactive small molecules, which have been frequently used in the drug development of various targets (Ma et al., 2011). In this study, the primary objective was to discover KRAS^{G12D} inhibitors through structure-based pharmacophore modeling and virtual screening. First, a pharmacophore model based on KRAS^{G12D} crystal structure was constructed and used as a three-dimensional (3D) search query to retrieve potential inhibitors from commercial databases. Then the recovered hit compounds were filtered through molecular docking research to refine the hits. Finally, the four screened compounds showed sub-nanomolar affinities for KRAS^{G12D} and had a dose-dependent inhibitory effect on human pancreatic cancer cells. Among them, the hit compound 3 was the most promising compound with a significant inhibitory effect on tumor growth in mice.

2 Materials and methods

2.1 Materials

Human pancreatic cancer cell line (Panc 04.03) was obtained from American Type Culture Collection (ATCC) (Manassas, VA, United States) and cultured in Dulbecco's modified Eagle's medium (DMEM) with 1% penicillin-streptomycin and 10% fetal bovine serum (FBS) in a humidified atmosphere, 5% CO₂ at 37°C. KRAS^{G12D} was purchased from Abcam (Cambridge, MA, United States). Hit compounds were purchased from WuXi AppTec.

2.2 Pharmacophore model generation

The virtual screening (VS.) method is designed to search large libraries of compounds *in silico*. The hit rate is usually much higher than traditional high throughput screening (HTS) (Tang et al., 2006; Shekhar, 2008). The crystal structure of KRAS^{G12D} (PDB ID: 7EWB) with a high resolution of 1.99 Å was downloaded from the Protein Data Bank (PDB) database and pretreated with the molecular operating environment (MOE) (Scholz et al., 2015) by removing water molecules, adding hydrogen atoms, and optimizing the orientation of hydrogen atoms. Based on the analysis of the interaction between the ligand and the amino acids in the KRAS^{G12D} active site, pharmacophore features were manually added using the pharmacophore editor of MOE (Nevin et al., 2012).

2.3 Virtual screening approach

An in-house chemical database contains 35,000 compounds with diverse structures and covers most of the chemical space, which is conducive to finding new skeleton molecules. The two-dimensional (2D) chemical structures of molecules in the database were firstly converted to 3D structures using the energy minimization algorithm of MOE software (MMFF94x force field) (Zheng et al., 2021). Through the pharmacophore search tool of the MOE (Zhang et al., 2020), all the compounds in the database were then screened according to the pharmacophore model, and the best-match hit compounds were evaluated using the root mean square distance (RMSD) values (The lower the RMSD values, the better the match). Finally, the hit compounds with an RMSD value of less than 0.09 Å were filtered by the molecular docking and the pharmacokinetic (PK) properties.

2.4 Molecular docking

Molecular docking was carried out through MOE software to evaluate the interaction between the hits of virtual screening and the active sites of KRAS^{G12D} (Scarpino et al., 2018). The crystal structure file of KRAS^{G12D} (PDB-ID:7EWB) was prepared for the docking studies where: 1) hydrogen atoms were added and water molecules were removed; 2) the partial charges were computed using Amber99 force field. The bound inhibitor TH-Z835 was used as the template to define the docking-active site in the crystal structure of KRAS^{G12D}. Molecular docking was performed in the active site using the triangle matcher algorithm. Docking scores were calculated through the dG scoring function of MOE software. The lower docking score indicated better binding affinity between KRAS^{G12D} and ligand (Zheng et al., 2021).

2.5 In silico pharmacokinetic studies

In silico prediction of the pharmacokinetic (PK) properties of the hit compounds was performed by the ADMETlab tool (Mohammed, 2021). In these calculations, using reference 3144, we evaluated the common PK parameters such as the molecular weight ($\text{mol_MW} \leq 800$), number of hydrogen bond donors ($\text{nHD} \leq 5$), number of hydrogen bond acceptors ($\text{nHA} \leq 10$), number of rotatable bonds ($\text{nRot} \leq 10$), the aqueous solubility ($-7 \leq \log S \leq 0.5$), topological polar surface area ($\text{TPSA} \leq 140$), caco-2 permeability ($\text{CP} \geq -5.15$), MDCK permeability, human intestinal absorption (HIA), $F_{20\%}$, $F_{30\%}$, volume of distribution (L/kg), $T_{1/2}$, rat oral acute toxicity, eye corrosion, and eye irritation.

2.6 Microscale thermophoresis (MST) experiments

MST is an effective method to evaluate biomolecular interactions and has been used to study the interactions between binding partners of different molecular sizes (Wienken et al., 2010; Seidel et al., 2013). According to the previously reported method to measure the interaction between small molecule inhibitors and KRAS^{G12D} protein, the MST assay was performed using Monolith NT.115 instrument (NanoTemp Technologies, GmbH, Munich, Germany) (Wienken et al., 2010). The red fluorescent dye was used for KRAS^{G12D} fluorescent labeling. Small molecule inhibitors were diluted 1:1 and titrated. The binding buffer (50 mM Tris, 230 mM NaCl) was added to the dilution curve of the small molecule inhibitors and the labeled protein. The final sample was centrifuged at 13,000 rpm for 10 min, and then filled into the capillary tube for MST analysis with 20% LED power and 50% MST power at room temperature. The equilibrium dissociation constant (K_d) was calculated using Nano Temper Analysis software.

2.7 MTT cell proliferation assay

According to the previously reported method (Yang et al., 2019), the human pancreatic cancer cell line (Panc 04.03) was seeded at the density of 2.4×10^4 on 96-well plates. After incubation at 37°C with 5% CO₂ for 24 h, the cells were incubated with different concentrations of inhibitors under the same conditions. After 72 h, MTT (0.5 mg/ml, 100 μ l) was added after the supernatant was discarded. Then keep the 96-well plate at 37°C for 4 h. After that, abandon the medium and inject 200 μ l of dimethyl sulfoxide (DMSO) into each well. The spectrophotometric absorbance of the sample at 570 nm was measured using a Synergy 4 Microplate Reader (BioTek Instruments Inc., United States). All of the compounds were tested three times in each of the cells.

2.8 In vivo anticancer activity

Based on previously reported protocols for investigating inhibition *in vivo* (Zhou et al., 2022), we injected Panc 04.03 cells (200 μ l, 1×10^7 cells) in the subdermal space on the right flank of 6-week-old BALB/c nude mice (Changzhou Cavens Laboratory Animal Co., Ltd, China). All experimental protocols were approved by the Animal Ethics Committee of China Pharmaceutical University (Ethical approval number: 2022-11-001). Once tumors grew to 80–100 mm³, mice were randomly divided into three groups (5 mice per group) and intraperitoneally administered with vehicle, hit compound 3 (3 mg/kg) and hit compound 3 (10 mg/kg) every 4 days for a total of five times. Tumor volume and body weight were measured every 4 days. Tumor volume was calculated using the formula $(c \times c \times d)/2$ (c , the smallest diameter; d , the largest diameter).

3 Results

3.1 Generation of pharmacophore model

The high-resolution X-ray structure of KRAS^{G12D} (PDB ID: 7EWB) in complex with the ligand TH-Z835 was downloaded from the PDB database. The generated structure-based pharmacophore model included four features (Figure 2): two aromatic features (F1 and F2: Aro) and two hydrogen-bond donor features (F3 and F4: Don). The two aromatic features of the pharmacophore model could be mapped onto the naphthalene ring of TH-Z835, which formed hydrophobic interactions with hydrophobic amino acids including Phe78, Met72, Val9 and Ala11. In addition, its hydrogen-bond donor features could match the nitrogen atoms of TH-Z835 that showed multiple hydrogen-bond interactions with Gly60, Glu62, Asp12, and His95. The above results reveal that this model may predict the spatial pharmacophore features of KRAS^{G12D} inhibitors.

3.2 Virtual screening

Figure 3 showed the virtual screen scheme that has been successfully used to identify inhibitors in other enzyme systems like Poly (ADP-Ribose) Polymerase-1 (PARP-1) (Zhou et al., 2019) and Tubulin (Zheng et al., 2021). MOE software was used for each step of virtual screening and molecular docking. Firstly, 35,000 compounds in the in-house chemical database were preliminarily screened according to the generated pharmacophore model of KRAS^{G12D}. Then, 69 compounds with an RMSD value of less than 0.09 Å were selected for the docking-base screening. Before molecular docking, it is very necessary to verify the reliability of docking. In this study, we

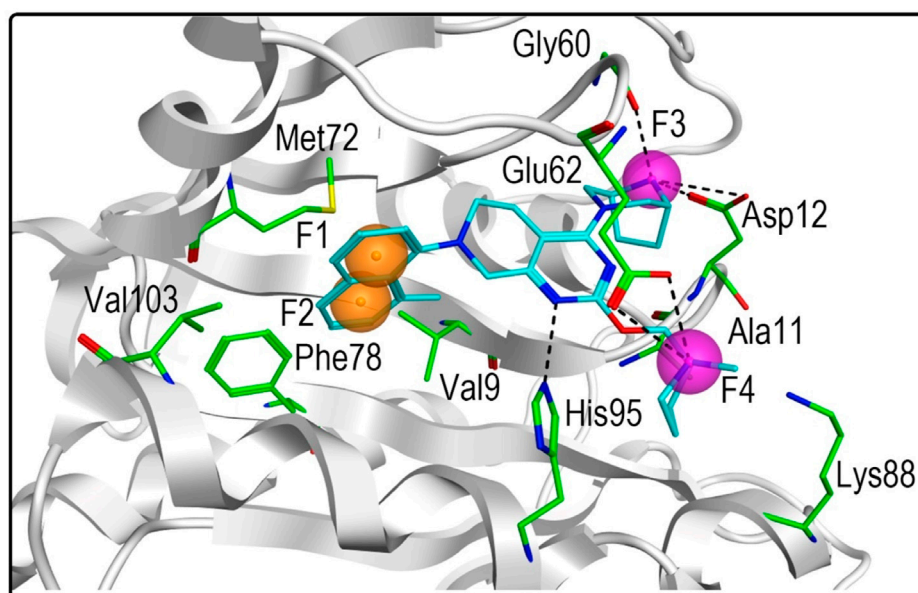


FIGURE 2

Pharmacophore model of KRAS^{G12D} was derived from the interaction of TH-Z835 and active-site amino acids. The ligand TH-Z835 is shown as cyan stick. Orange spheres correspond to aromatic features (F1 and F2: Aro), and purple spheres represent hydrogen-bond donors (F3 and F4: Don). Active-site residues are shown as green sticks. Hydrogen bonds are represented by black dotted lines.

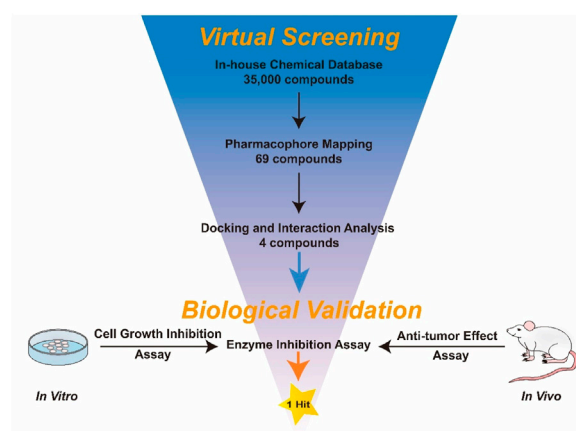


FIGURE 3

Schematic diagram of virtual screening and biological evaluation adopted in this study.

used the ligand (TH-Z835) of the crystal structure KRAS^{G12D}-TH-Z835 complex (PDB ID: 7EWB) as the template for verification. The co-crystallized ligand TH-Z835 was re-docked in the active site of KRAS^{G12D} (Figure 4A). We can observe that the docking conformation of TH-Z835 was well mapped with the actual conformation in the active site, indicating the good

reliability of the docking method. Thus, this verified docking method can be used in virtual screening.

Next, 69 selected compounds of pharmacophore-base screening were docked into the KRAS^{G12D} binding site. TH-Z835 was used as the positive control and has a docking score of -10.04 kcal/mol. Based on docking scores, four top compounds (namely, hit compounds 1–4) below -10.04 kcal/

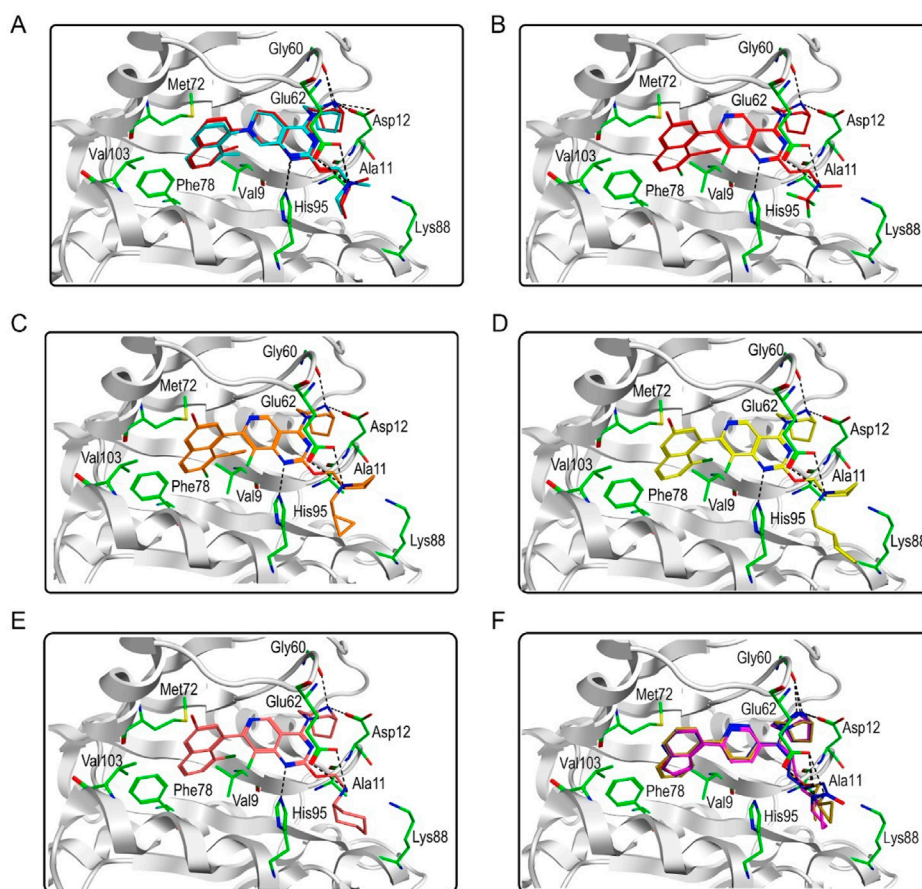


FIGURE 4

Predicted binding modes. (A) The docking conformation (red) and the actual conformation (cyan) of the co-crystallized ligand TH-Z835; (B) Hit compound 1; (C) Hit compound 2; (D) Hit compound 3; (E) Hit compound 4; (F) Hit compounds 5–7.

mol and other three hit compounds (namely, hit compounds 5–7) ranking below them were further selected for predicting the three-dimensional interaction modes. Similar to TH-Z835, hit compounds 1–4 exhibited hydrogen-bond interactions with the key amino acids in the active site including His95, Glu62, Gly60, and Asp12 (Figures 4B–E). However, other hit compounds 5–7 could not form a hydrogen-bond interaction with His95 (Figure 4F). Compared with TH-Z835, halogen atoms in the skeleton of hit compounds 1–4 not only could exhibit stronger hydrophobic interactions with Val9, but also could greatly increase molecular liposolubility and metabolic stability. The chemical structures of all the hit compounds 1–7 were shown in Figure 5. In addition, a good pharmacophore mapping with the hit compounds 1–4 on the model was shown in Figure 6. The naphthalene ring of each hit could match the aromatic features of F1 and F2, while its nitrogen atoms were mapped onto the hydrogen-bond donor features of F3 and F4 respectively.

To provide a reliable pharmacokinetic (PK) property of a compound, *in silico* prediction of the PK properties of these four hit compounds were carried out using the reference inhibitor 3144 as reference (Table 1). In this calculation, we evaluated these common PK parameters including the molecular weight ($\text{mol_MW} \leq 800$), number of hydrogen bond donors ($\text{nHD} \leq 5$), number of hydrogen bond acceptors ($\text{nHA} \leq 10$), number of rotatable bonds ($\text{nRot} \leq 10$), the aqueous solubility ($-7 \leq \log S \leq 0.5$), topological polar surface area ($\text{TPSA} \leq 140$), caco-2 permeability ($\text{CP} \geq -5.15$), MDCK permeability, human intestinal absorption (HIA), $F_{20\%}$, $F_{30\%}$, volume of distribution (L/kg), $T_{1/2}$, rat oral acute toxicity, eye corrosion, and eye irritation. The result indicated that these parameter values of the hit compounds 1–4 are in the appropriate range. However, the reference inhibitor 3144 exceeded the specified range of nRot and caco-2 permeability respectively. Therefore, based on the molecular interaction and PK analysis, the four candidate hits (hit compounds 1–4) were finally chosen for further biological evaluation.

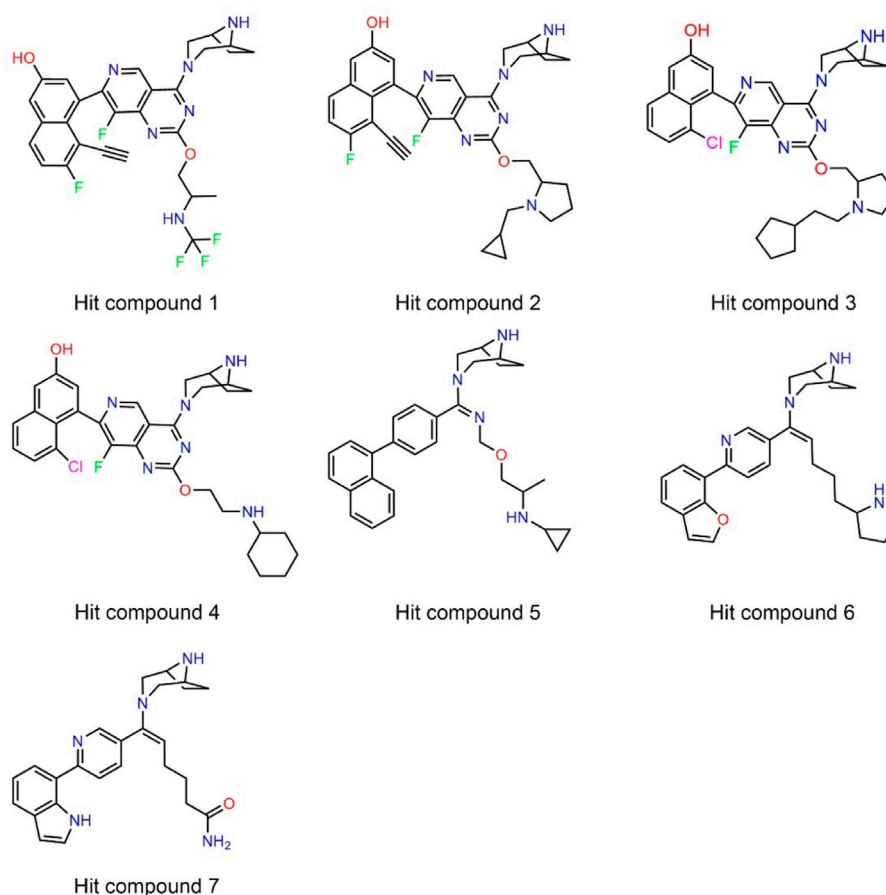


FIGURE 5
The chemical structures of hit compounds 1–7.

3.3 MST

Microscale Thermophoresis (MST) is a general method for quantifying binding affinity by measuring the equilibrium dissociation constant (K_d) (Bartoschik et al., 2018). The MST binding assays showed that hits 1–4 effectively bound to the KRAS^{G12D} in the sub-nanomolar range ($K_d = 0.13$ – 0.98 nM) and displayed a stronger binding affinity for KRAS^{G12D} compared with the positive control TH-Z835 (Table 2).

3.4 Cell growth inhibitory activity

In this experiment, the MTT method was used to detect the effects of hit compounds 1–4 on the proliferation of human pancreatic cancer cells (Panc 04.03). The results showed that hits 1–4 had a dose-dependent effect on the proliferation of Panc 04.03 cells (Figure 7). In addition, their IC_{50} values were further calculated. Compared with other hits and the positive control

TH-Z835, hit 3 with the IC_{50} value of 43.80 nM exhibited a stronger anti-proliferative activity on Panc 04.03 cells. Therefore, hit compound 3 was selected as a lead compound and further used for anti-tumor experimental evaluation *in vivo*.

3.5 Tumor growth inhibition *in vivo*

Given the significant inhibitory effect of hit compound 3 on pancreatic cancer cell growth *in vitro*, the anti-pancreatic cancer activity of hit compound 3 was evaluated. The mice were randomly divided into three groups (5 mice per group): the vehicle control group, hit compound 3 (3 mg/kg) treated group and hit compound 3 (10 mg/kg) treated group. The hit compound 3 significantly inhibited the growth of Panc 04.03 in a concentration-dependent manner after intraperitoneal injection for 20 days. As shown in Figure 8, the growth rate of xenograft tumors in BALB/c nude mice after hit compound 3 administration was significantly reduced

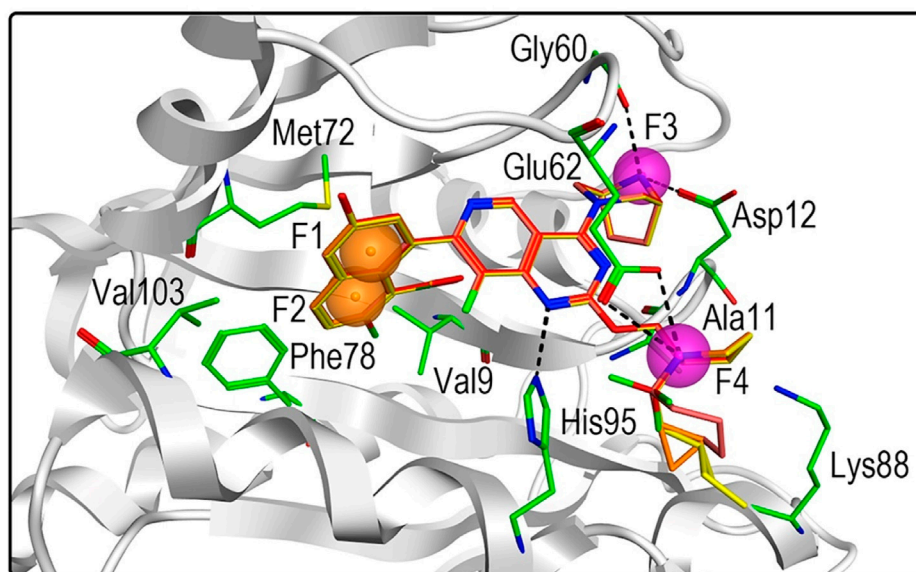


FIGURE 6

Three-dimensional pharmacophore mapping of hit compounds 1–4 with the active-site residues in KRAS^{G12D}. Orange spheres correspond to aromatic features (F1 and F2: Aro), and purple spheres represent hydrogen-bond donors (F3 and F4: Don).

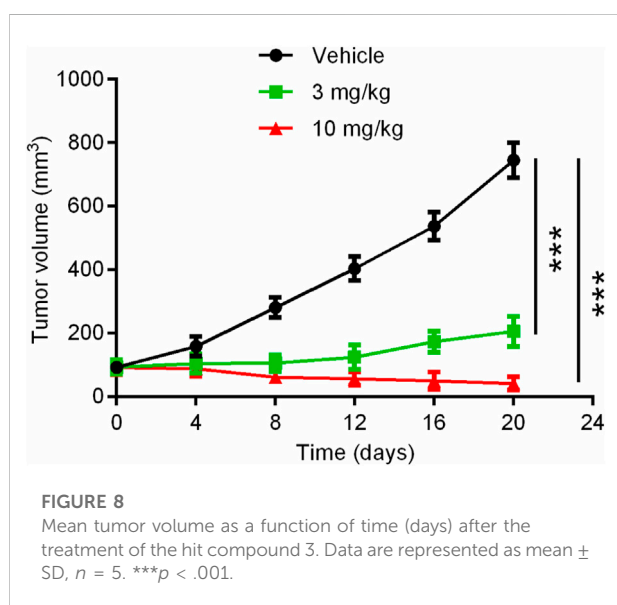
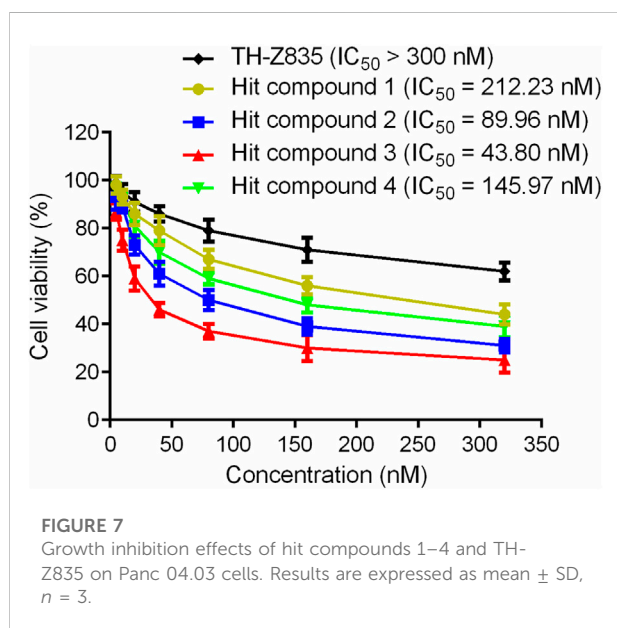
TABLE 1 Pharmacokinetic profile of the four hit compounds and reference 3144.

Profile	Compounds				
	Hit compound 1	Hit compound 2	Hit compound 3	Hit compound 4	3144
Molecular Weight (MW)	584.200	596.270	630.290	576.240	716.260
nHA	8	8	8	8	8
nHD	3	2	2	3	4
nRot	7	7	8	7	13
TPSA	95.430	86.640	86.640	95.430	87.790
logS	-6.016	-5.298	-5.329	-6.154	-4.822
Caco-2 Permeability (log unit)	-4.994	-4.906	-5.036	-5.124	-5.716
MDCK Permeability	1.7e-05	9.8e-06	1.2e-05	1.5e-05	5.1e-06
HIA	—	—	—	—	—
F _{20%}	—	—	—	—	—
F _{30%}	—	—	—	—	—
Volume of distribution (L/kg)	2.424	2.525	2.316	2.182	3.454
T _{1/2}	.024	.015	.013	.020	.005
Rat Oral Acute Toxicity	—	—	—	—	—
Eye Corrosion	—	—	—	—	—
Eye Irritation	—	—	—	—	—

TABLE 2 The docking scores and biological data of four hits.

Name	Docking score [kcal/mol]	K_d (nM)	IC_{50} (nM) ^a
Hit compound 1	-11.56	$0.98 \pm .09$	212.23
Hit compound 2	-11.69	$0.46 \pm .08$	89.96
Hit compound 3	-11.75	$0.13 \pm .05$	43.80
Hit compound 4	-11.61	$0.76 \pm .11$	145.97
TH-Z835	-10.04	$1.08 \pm 0.07 \mu\text{M}$	>300

^a IC_{50} (nM) is the concentration of compound needed to inhibit cell growth by 50% following 72 h cell treatment with hit compounds 1-4 and TH-Z835, respectively.



compared with the untreated group. In addition, the significant difference in tumor volume between the untreated and treated groups further demonstrated the inhibitory effect of hit compound 3 on xenograft tumor growth in BALB/c nude mice *in vivo*.

4 Discussion and conclusion

In order to develop inhibitors of KRAS^{G12D}, the most common KRAS mutant in pancreatic cancer, we used a structure-based screening method to successfully identify four hit compounds and evaluated their activity *in vitro* and *in vivo*. The MST experimental result showed that hits 1-4 had sub-nanomolar affinities for KRAS^{G12D}. Particularly, hit compound 3 had a remarkable anti-proliferation effect on human pancreatic cancer cells and significantly inhibited tumor growth in tumor-bearing mice. Since hit compound 3 is the most promising lead compound targeting KRAS^{G12D}, structural optimization of hit compound 3 is currently under way in our laboratory to further explore structurally novel and more effective KRAS^{G12D} inhibitors. In addition, the results of this experiment prove that this screening scheme provides guidance in identifying potent KRAS^{G12D} inhibitors, and may be applicable to other KRAS family members in the future.

Data availability statement

The original contributions presented in the study are included in the article/Supplementary Material, further inquiries can be directed to the corresponding authors.

Ethics statement

The animal study was reviewed and approved by all experimental protocols were approved by the Animal Ethics Committee of China Pharmaceutical University.

Author contributions

Conceptualization, YZ, YQ, and M-MN; methodology, YW, JL, and M-MN; formal analysis, YW, HZ, and JL; writing original draft preparation, YW, HZ, and YZ; writing-review and editing, YQ. All authors read and approved the final manuscript.

Funding

The study was supported by Youth Program in Science & Technology of Qing Miao Talent Program of Changzhou Health Committee (No. CZQM2022010), Changzhou Health Committee (No. QN202026), and Changzhou Sci & Tech Program (No. CJ20200055).

References

- Bartoschik, T., Galinec, S., Kleusch, C., Walkiewicz, K., Breitsprecher, D., Weigert, S., et al. (2018). Near-native, site-specific and purification-free protein labeling for quantitative protein interaction analysis by MicroScale Thermophoresis. *Sci. Rep.* 8 (1), 4977. doi:10.1038/s41598-018-23154-3
- Bazhin, A. V., Shevchenko, I., Umansky, V., Werner, J., and Karakhanova, S. (2014). Two immune faces of pancreatic adenocarcinoma: Possible implication for immunotherapy. *Cancer Immunol. Immunother.* 63 (1), 59–65. doi:10.1007/s00262-013-1485-8
- Busato, D., Mossenta, M., Dal Bo, M., Macor, P., and Toffoli, G. (2022). The proteoglycan glypican-1 as a possible candidate for innovative targeted therapeutic strategies for pancreatic ductal adenocarcinoma. *Int. J. Mol. Sci.* 23 (18), 10279. doi:10.3390/ijms231810279
- Buscail, L., Bournet, B., and Cordelier, P. (2020). Role of oncogenic KRAS in the diagnosis, prognosis and treatment of pancreatic cancer. *Nat. Rev. Gastroenterol. Hepatol.* 17 (3), 153–168. doi:10.1038/s41575-019-0245-4
- Chen, H., Smail, J. B., Liu, T., Ding, K., and Lu, X. (2020). Small-molecule inhibitors directly targeting KRAS as anticancer therapeutics. *J. Med. Chem.* 63 (23), 14404–14424. doi:10.1021/acs.jmedchem.0c01312
- Cox, A. D., Fesik, S. W., Kimmelman, A. C., Luo, J., and Der, C. J. (2014). Drugging the undruggable RAS: Mission possible? *Nat. Rev. Drug Discov.* 13 (11), 828–851. doi:10.1038/nrd4389
- Ducreux, M., Cuhna, A. S., Caramella, C., Hollebecque, A., Burtin, P., Goere, D., et al. (2015). Cancer of the pancreas: ESMO clinical practice guidelines for diagnosis, treatment and follow-up. *Ann. Oncol.* 26 (5), v56–v68. doi:10.1093/annonc/mdv295
- Eibl, G., and Rozengurt, E. (2019). KRAS, yap, and obesity in pancreatic cancer: A signaling network with multiple loops. *Semin. Cancer Biol.* 54, 50–62. doi:10.1016/j.semcancer.2017.10.007
- Elsayed, M., and Abdelrahman, M. (2021). The latest advancement in pancreatic ductal adenocarcinoma therapy: A review article for the latest guidelines and novel therapies. *Biomedicine* 9 (4), 389. doi:10.3390/biomedicine9040389
- Grasso, C., Jansen, G., and Giovannetti, E. (2017). Drug resistance in pancreatic cancer: Impact of altered energy metabolism. *Crit. Rev. Oncol. Hematol.* 114, 139–152. doi:10.1016/j.critrevonc.2017.03.026
- He, Q., Liu, Z., and Wang, J. (2022). Targeting KRAS in pdac: A new way to cure it? *Cancers (Basel)* 14 (20), 4982. doi:10.3390/cancers14204982
- Kargbo, R. B. (2022). Long-awaited small-molecule drug candidate for drugging the next undruggable KRAS(G12D) mutant in cancer therapy. *ACS Med. Chem. Lett.* 13 (5), 773–774. doi:10.1021/acsmchemlett.2c00154
- Kessler, D., Gmachl, M., Mantoulidis, A., Martin, L. J., Zoephel, A., Mayer, M., et al. (2019). Drugging an undruggable pocket on KRAS. *Proc. Natl. Acad. Sci. U. S. A.* 116 (32), 15823–15829. doi:10.1073/pnas.1904529116
- Khan, I., Rhett, J. M., and O'Bryan, J. P. (2020). Therapeutic targeting of RAS: New hope for drugging the "undruggable. *Biochim. Biophys. Acta Mol. Cell Res.* 1867 (2), 118570. doi:10.1016/j.bbamcr.2019.118570

Conflict of interest

The authors declare that the research was conducted in the absence of any commercial or financial relationships that could be construed as a potential conflict of interest.

Publisher's note

All claims expressed in this article are solely those of the authors and do not necessarily represent those of their affiliated organizations, or those of the publisher, the editors and the reviewers. Any product that may be evaluated in this article, or claim that may be made by its manufacturer, is not guaranteed or endorsed by the publisher.

- Kimmelman, A. C. (2015). Metabolic dependencies in RAS-driven cancers. *Clin. Cancer Res.* 21 (8), 1828–1834. doi:10.1158/1078-0432.CCR-14-2425
- Landman, B. A., Allen, J. R., Allen, J. G., Amegadzie, A. K., Ashton, K. S., Booker, S. K., et al. (2020). Discovery of a covalent inhibitor of KRAS(G12C) (AMG 510) for the treatment of solid tumors. *J. Med. Chem.* 63 (1), 52–65. doi:10.1021/acs.jmedchem.9b01180
- Ma, D.-L., Chan, D. S.-H., and Leung, C.-H. (2011). Molecular docking for virtual screening of natural product databases. *Chem. Sci.* 2 (9), 1656–1665. doi:10.1039/c1sc00152c
- Mao, Z., Xiao, H., Shen, P., Yang, Y., Xue, J., Yang, Y., et al. (2022). KRAS(G12D) can be targeted by potent inhibitors via formation of salt bridge. *Cell Discov.* 8 (1), 5. doi:10.1038/s41421-021-00368-w
- Mohammed, I. J. A. P. A. (2021). *Virtual screening of Microalgal compounds as potential inhibitors of Type 2 Human Transmembrane serine protease (TMPRSS2).*
- Morris, J. P. t., Wang, S. C., and Hebrok, M. (2010). KRAS, Hedgehog, Wnt and the twisted developmental biology of pancreatic ductal adenocarcinoma. *Nat. Rev. Cancer* 10 (10), 683–695. doi:10.1038/nrc2899
- Nevin, D. K., Peters, M. B., Carta, G., Fayne, D., and Lloyd, D. G. (2012). Integrated virtual screening for the identification of novel and selective peroxisome proliferator-activated receptor (PPAR) scaffolds. *J. Med. Chem.* 55 (11), 4978–4989. doi:10.1021/jm300068n
- Peng, J., Li, Y., Zhou, Y., Zhang, L., Liu, X., and Zuo, Z. (2018). Pharmacophore modeling, molecular docking and molecular dynamics studies on natural products database to discover novel skeleton as non-purine xanthine oxidase inhibitors. *J. Recept. Signal Transduct. Res.* 38 (3), 246–255. doi:10.1080/10799893.2018.1476544
- Salem, M., El-Refai, S., Sha, W., Grothey, A., Puccini, A., George, T., et al. (2021). O-3 Characterization of KRAS mutation variants and prevalence of KRAS-G12C in gastrointestinal malignancies. *Ann. Oncol.* 32, S218. doi:10.1016/j.annonc.2021.05.007
- Scarpino, A., Ferenczy, G. G., and Keseru, G. M. (2018). Comparative evaluation of covalent docking tools. *J. Chem. Inf. Model* 58 (7), 1441–1458. doi:10.1021/acs.jcim.8b00228
- Scholz, C., Knorr, S., Hamacher, K., and Schmidt, B. (2015). DOCKTITE—a highly versatile step-by-step workflow for covalent docking and virtual screening in the molecular operating environment. *J. Chem. Inf. Model* 55 (2), 398–406. doi:10.1021/ci500681r
- Seidel, S. A., Dijkman, P. M., Lea, W. A., van den Bogaart, G., Jerabek-Willemsen, M., Lasic, A., et al. (2013). Microscale thermophoresis quantifies biomolecular interactions under previously challenging conditions. *Methods* 59 (3), 301–315. doi:10.1016/j.ymeth.2012.12.005
- Shekhar, C. (2008). *In silico pharmacology: Computer-aided methods could transform drug development.* *Chem. Biol.* 15 (5), 413–414. doi:10.1016/j.chembiol.2008.05.001
- Simanshu, D. K., Nissley, D. V., and McCormick, F. (2017). RAS proteins and their regulators in human disease. *Cell* 170 (1), 17–33. doi:10.1016/j.cell.2017.06.009

- Sung, H., Ferlay, J., Siegel, R. L., Laversanne, M., Soerjomataram, I., Jemal, A., et al. (2021). Global cancer statistics 2020: GLOBOCAN estimates of incidence and mortality worldwide for 36 cancers in 185 countries. *CA Cancer J. Clin.* 71 (3), 209–249. doi:10.3322/caac.21660
- Tang, Y., Zhu, W., Chen, K., and Jiang, H. (2006). New technologies in computer-aided drug design: Toward target identification and new chemical entity discovery. *Drug Discov. Today Technol.* 3 (3), 307–313. doi:10.1016/j.ddtec.2006.09.004
- Vasta, J. D., Peacock, D. M., Zheng, Q., Walker, J. A., Zhang, Z., Zimprich, C. A., et al. (2022). KRAS is vulnerable to reversible switch-II pocket engagement in cells. *Nat. Chem. Biol.* 18 (6), 596–604. doi:10.1038/s41589-022-00985-w
- Wang, S., Zheng, Y., Yang, F., Zhu, L., Zhu, X. Q., Wang, Z. F., et al. (2021). The molecular biology of pancreatic adenocarcinoma: Translational challenges and clinical perspectives. *Signal Transduct. Target Ther.* 6 (1), 249. doi:10.1038/s41392-021-00659-4
- Welsch, M. E., Kaplan, A., Chambers, J. M., Stokes, M. E., Bos, P. H., Zask, A., et al. (2017). Multivalent small-molecule pan-RAS inhibitors. *Cell* 168 (5), 878–889. doi:10.1016/j.cell.2017.02.006
- Wienken, C. J., Baaske, P., Rothbauer, U., Braun, D., and Duhr, S. (2010). Protein-binding assays in biological liquids using microscale thermophoresis. *Nat. Commun.* 1, 100. doi:10.1038/ncomms1093
- Yang, D. S., Yang, Y. H., Zhou, Y., Yu, L. L., Wang, R. H., Di, B., et al. (2019). A redox-triggered bispecific supramolecular nanomedicine based on peptide self-assembly for high-efficacy and low-toxic cancer therapy. *Adv. Funct. Mater.* 30 (4), 1904969. doi:10.1002/adfm.201904969
- Zhang, Y., Zhang, T. J., Tu, S., Zhang, Z. H., and Meng, F. H. (2020). Identification of novel src inhibitors: Pharmacophore-based virtual screening, molecular docking and molecular dynamics simulations. *Molecules* 25 (18), 4094. doi:10.3390/molecules25184094
- Zheng, L., Ren, R., Sun, X., Zou, Y., Shi, Y., Di, B., et al. (2021). Discovery of a dual Tubulin and poly(ADP-ribose) polymerase-1 inhibitor by structure-based pharmacophore modeling, virtual screening, molecular docking, and biological evaluation. *J. Med. Chem.* 64 (21), 15702–15715. doi:10.1021/acs.jmedchem.1c00932
- Zheng, Q., Peacock, D. M., and Shokat, K. M. (2022). Drugging the next undruggable KRAS allele-Gly12Asp. *J. Med. Chem.* 65 (4), 3119–3122. doi:10.1021/acs.jmedchem.2c00099
- Zhou, C. Y., Dong, Y. P., Sun, X., Sui, X., Zhu, H., Zhao, Y. Q., et al. (2018). High levels of serum glypican-1 indicate poor prognosis in pancreatic ductal adenocarcinoma. *Cancer Med.* 7 (11), 5525–5533. doi:10.1002/cam4.1833
- Zhou, Y., Tang, S., Chen, T., and Niu, M. M. (2019). Structure-based pharmacophore modeling, virtual screening, molecular docking and biological evaluation for identification of potential poly (ADP-Ribose) polymerase-1 (PARP-1) inhibitors. *Molecules* 24 (23), 4258. doi:10.3390/molecules24234258
- Zhou, Y., Zou, Y., Yang, M., Mei, S., Liu, X., Han, H., et al. (2022). Highly potent, selective, biostable, and cell-permeable cyclic d-peptide for dual-targeting therapy of lung cancer. *J. Am. Chem. Soc.* 144 (16), 7117–7128. doi:10.1021/jacs.1c12075